Sensors & Transducers, Vol. 225, Issue 9, September 2018, pp. 63-68

Sensors & Transducers
Published by IFSA Publishing, S. L., 2018
http://www.sensorsportal.com

Design of a Low Voltage, Low Power Array Readout Circuit for Liquid Crystal Chemical and Biological Sensors

Alireza Hassanzadeh
Electrical Eng. Dept. Shahid Beheshti University, 1983963113, Iran
Tel.: +9821 29904091, fax: +982122431804
E-mail: a_hassanzadeh@sbu.ac.ir

Received: 19 August 2018 /Accepted: 20 September 2018 /Published: 30 September 2018

Abstract: In this paper a new low power, low voltage CMOS read out circuit has been designed to interface array of liquid crystal chemical and biological sensors. Liquid crystal (LC) has been a promising sensor for detection of chemical and biological agents. Low contamination of chemical agents can be amplified using liquid crystal molecules. Array sensors reduce risk of false detection of low ppm agent presence. The designed circuit uses a low voltage, low frequency capacitance to time conversion technique in a differential sensor structure. Auto zero and offset cancellation are easily implemented in the design using a digital programmable counter circuit. The designed chip uses 5.5 μm^2 of chip area per channel and consumes 0.2 µW of power from a single 0.5 V supply.

Keywords: Liquid crystal sensor, Capacitive transduction, Chemical and biological sensors, Interface circuit, Low power.

1. Introduction

Liquid Crystal (LC) sensor has been used to detect low contamination of chemical and biological agents. LC molecules can amplify small changes at the surface to large molecule orientation change in the crystal structure. LC sensor has been used to detect mustard gas, West Nile and Influenza viruses and protein bindings. Researchers in reference [1] and [2] used optical transduction for LC molecule change detection. Although, optical detection method has proved effective, but it requires transparent substrate and it is difficult for field deployment. A method developed in references [3] and [4] uses capacitive transduction to detect LC molecule orientation change. If array of sensors is used false alarms can be minimized. Some sensors may detect presence of agents with error, but a collective decision can be made when array of sensors are used for detection. An interface CMOS circuit had been developed in reference [5] that uses a differential charge amplifier for detection of small capacitance change of a differential LC sensor. Even though, the circuit offers very high accuracy capacitance measurement, large circuit area limits array implementation. Large area electronic circuits can be developed on amorphous hydrogenated silicon. The circuit in [6] uses a-Si:H transistors to interface LC sensors for large array as large as an iPad display. However, a-Si:H transistors have low electron mobility and poor matching properties. Furthermore, only NMOS transistors are available in a-Si:H technology with high mobility that limits circuit design flexibility. The circuit developed in this paper uses a low voltage direct capacitance to time conversion technique in a differential sensor structure. The low voltage circuit meets Friedrich's voltage requirements for the LC sensor. The interface circuit uses a single 0.5 V supply voltage with auto zero and offset cancellation capability.

This paper has been arranged as follows. Section 2, explains LC sensor and capacitance transduction technique. In Section 3, the proposed circuit and its specifications are explained. Simulation waveforms and discussions are in Section 4. Concluding remarks are at the end.

2. Liquid Crystal Sensor and Capacitive Transduction

Liquid Crystal is a phase of material between crystalline solid and isotropic liquid. The shapes of LC molecules are rod-like (calamitic) or disk-like (discotic). Because of asymmetrical shapes, these molecules show different properties in different directions. Fig. 1 shows liquid crystal molecules. Lyotropic and thermotropic are two types of LC materials. The phase of LC changes with concentration change in Lyotropic materials. Thermotropic phase changes with respect to temperature change. Fig. 2 shows different phases of LC thermotropic material with temperature change [2, 7].

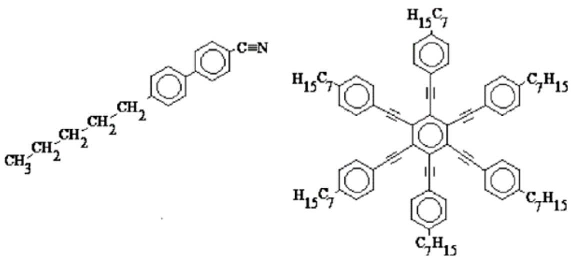

Fig. 1. Liquid Crystal anisotropic molecules (rod-like and disk-like) [7].

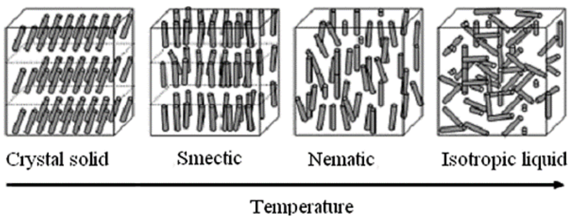

Fig. 2. Phase change of thermotropic LC material with temperature change [7].

As shown in Fig. 2, when temperature is low molecules are in solid form and have similar orientation. As temperature increases molecules lose their orientation and move in place. In the Nematic phase, molecules move freely, but keep long range orientation order. As temperature increases higher, since molecules move randomly, the material becomes isotropic. The Nematic phase is a good candidate for detection of chemical and biological agents, since molecules can amplify small changes at the surfaces when chemical agents exist. When LC molecules change orientation at the surface, other adjacent molecules try to follow the direction change that can amplify orientation change and small agent particles can be detected.

Average molecules orientation can be displayed using a vector axis ($\vec{n}$) as shown in Fig. 3. The anisotropic property of LC molecules shows different permittivity in different directions. The permittivity matrix is shown in equation (1), which has $\varepsilon_{\parallel}$ for electric field in parallel to the director axis and $\varepsilon_{\perp}$ for electric field normal to the director axis ($\vec{n}$).

$$\varepsilon_m = \varepsilon_0 \begin{pmatrix} \varepsilon_{\perp} & 0 & 0 \\ 0 & \varepsilon_{\perp} & 0 \\ 0 & 0 & \varepsilon_{\parallel} \end{pmatrix} \quad (1)$$

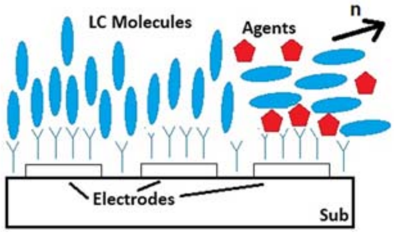

Fig. 3. LC orientation change when exposed to agents.

The difference between $\varepsilon_{\parallel}$ and $\varepsilon_{\perp}$ can be as high as 17.5 for BL006 a type of LC material. This large permittivity change, because of molecule orientation can be detected using electric field. Fig. 4 shows interdigitated micro-capacitive sensors that can be used to measure capacitance change caused by LC orientation change.

Fig. 4. Interdigitated capacitors built on glass substrate with gold fingers.

The finger spacing can be in submicron range and can be fabricated as instructed in reference [5]. Interdigitated capacitors can have LC and agent interface on top, while capacitance can be measured at the bottom. The top of interdigitated capacitor is treated with an alignment layer that keeps the initial orientation of LC molecules fixed. The LC is spin coated on the surface to provide a thin layer of LC material that is exposed to agents. Homeotropic and homogenous alignments are common for initial LC orientation, which are perpendicular and parallel to the surface of the sensor respectively. Fig. 3 shows interdigitated sensor electrodes with an alignment layer. When an agent is detected using LC molecules, the LC orientation changes as shown in Fig. 3. LC molecule orientation change can cause permittivity change in the LC capacitive sensor [3-4]. If electrode structure of capacitive sensor is known the capacitance can be calculated using Equation (2).

$$C = \frac{Q}{V} = \frac{\oint \vec{D}.d\vec{s}}{-\int \vec{E}.d\vec{l}}, \qquad (2)$$

where D is the displacement vector and E is the electric field. To consider any temperature change on sensors and other mismatch parameters for the capacitive sensor a differential structure is used. Both sensors are made completely the same and only one sensor is exposed to chemical agents. This method cancels out all similar parasitic parameters experienced by sensors and only agent presence causes capacitance difference.

3. LC Sensor Interface

In this section LC sensor requirements and interface circuit design are explained. LC capacitive sensor does not generate any electrical signal and some external excitation needs to be applied to the sensor for the measurement. Because of sensor material type, special treatment should be used for the interface circuit.

A. LC Sensor Excitation Requirements

Since LC capacitive sensors are passive components, excitation signal needs to be used for measuring sensor capacitance. Voltage excitation is normally used for capacitance measurement. Large electric fields can easily change LC orientation, the concept that is used for LC displays. In order to avoid any change in the LC orientation because of excitation signal, the electric field should be kept well below the Friedrich's voltage. This voltage is a few tenths of a volt. DC voltage cannot be used for LC excitation that causes charge migration. Therefore, AC excitation should be employed with small amplitude to avoid reorientation of the LC molecules. Best practice for LC excitation requirements have been investigated in reference [8]. Frequencies about 1 kHz has been shown to be a good range for measurement of LC sensors. To provide all voltage and excitation requirements a ramp signal has been used within the accepted frequency range. Single 0.5 V supply voltage has been used to design the interface circuit to avoid any large electric field on the LC sensor. In the next section circuit details and block diagrams are explained.

B. Block Diagram of the Interface Circuit

Many techniques have been published for integrated capacitance to digital conversion for MEMS based capacitive sensors. Among the methods Capacitance to Voltage conversion and using analog to digital conversion is a common method that consumes large power and chip area [9]. Switched Capacitor Sigma-Delta converters (SC-SD) avoid using large resistors and offer high resolution analog to digital conversion at low frequencies [5]. Capacitance to period or duty cycle conversion is simple method that easily converts capacitance to period, which can be converted to digital using a simple counter [10]. A method used in [11] uses two RC oscillators made of sensor and dummy capacitances and counters to convert capacitance to digital. The method used in this paper is based on Capacitance to Time conversion in a differential structure. For the proposed circuit used in this paper a differential structure has been used in the analog section as well as digital section of the interface circuit to cancel out any common parasitic parameter on circuit operation. Fig. 5 shows a block diagram of the interface circuit used for the LC capacitive sensor interface. Two interdigitated capacitors are used for differential measurement structure. One sensor is used as dummy and the other is the main active sensor that is exposed to chemical agents.

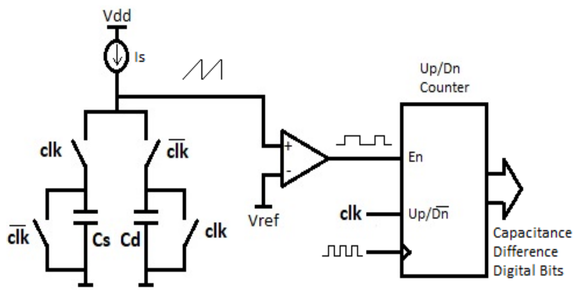

Fig. 5. Block diagram of the sensor interface.

A single current source is used for charging both sensors alternatingly using analog switches. The current source guarantees linear charge of the sensor capacitance. Using a current source is the most energy efficient way to charge a capacitor with low power dissipation. The time required to charge capacitors to a reference voltage is dependent on capacitance values. Capacitance charging time formulas is shown in (3).

$$T_{charge} = C \cdot V_{ref} / I_s, \qquad (3)$$

where T_{charge} is the charging time from zero to V_{ref}, C is the sensor's capacitance and I_s is the current source value. V_{ref} is used as reference voltage for the next stage comparator. Since a current source is used for charging capacitors, the output voltage will be a linear ramp. The current source is readily implemented by a transistor and current mirror. Because a single current source is used for charging both capacitors, matching of current sources is not required, if separate current sources were used. Current source value has been adjusted to provide acceptable voltage across sensor capacitances during clock periods. The output voltage of both sensors is compared with a single comparator and is converted to pulse width at the output of the comparator. Again using one comparator for both sensors avoids any mismatch in comparison circuit and comparator offset will be the same for both sensors. Dummy and active sensors are charged using the current source alternatively in every high and low state of each cycle of the clock signal. Therefore, the output low voltage of the comparator in each T/2 of cycle is proportional to capacitance value of active and dummy sensor. The clock signal *clk* is connected to the *Up/Dn* control of an 8-bit counter. Therefore, the counter counts up for active sensor time and counts down for dummy sensor pulse duration. In this way, the capacitance difference is directly obtained and a differential measurement is performed in digital form. The resolution of the counter and so the measurement value can be adjusted using counter clock frequency and the number of bits used for the counter. The propagation delay of the flip-flops used in the counter circuit determines maximum clock frequency that can be used for the counter. The counter output value is proportional to capacitance difference and can be adjusted for the required resolution. If the sensor is used for detection purposes only and resolution is not of great concern, the number of counter bits (number of flip-flops) can be minimized for power and area savings.

C. Auto Zero and Offset Cancellation

Two sensors have the same number of interdigitated fingers for capacitance measurement and both are treated similarly for orientation alignment to avoid any initial sensor mismatch. Even if the best practice has been used to match both LC capacitive sensors, because of the LC material and different thickness layers of LC or during operation while residual agents are present, some mismatch may still exist. To bring both sensors to the same value different techniques can be employed. In reference [5], number of sensor fingers has been adjusted using transistor switches to change capacitance value and remove sensor mismatch or offset. The fingers can be added using MOS transistors to change capacitance value. When sensor is exposed to chemical agents, some residue may remain on active sensor that needs to be adjusted and nulled for incremental measurements. For the proposed sensor interface, in order to avoid complexity of changing number of fingers in the sensor section, auto-zero and offset cancellation can be easily performed in the digital counter section. The current counter measurement value can be easily subtracted from the next clock phase measurement by preloading the current value into the Up/Dn counter. Therefore, the counter will count from the preload value and offset or auto-zero has been performed for the purpose. Fig. 6 shows block diagram of the offset cancellation and auto-zero phase.

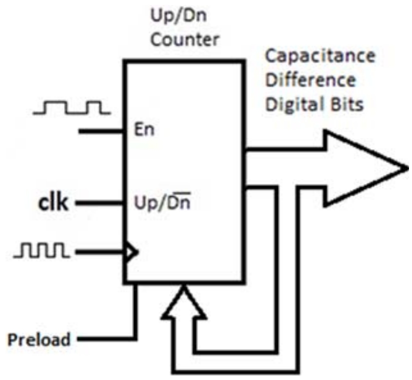

Fig. 6. Auto zero and offset cancellation.

D. CMOS Implementation

Fig. 7 shows CMOS circuit details of the interface circuit. The complete circuit uses 0.5 V supply voltage for all analog and digital interface circuits. Small supply voltage lowers power consumption of the circuit and provides proper voltage requirement for the LC sensor excitation. A pulse generator with adjustable frequency generates clock for *clk* and $\overline{clk}$ signals. A CMOS current mirror including M5 and M6 transistors generates 12 nA current for charging sensor capacitors. NMOS analog switches M2 and M3 have been used to steer current into sensor and dummy capacitors alternatively. Two other NMOS switches M1 and M4 discharge capacitors to zero voltage when the other capacitor is charging.

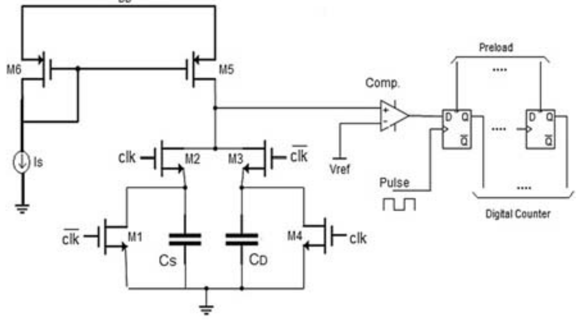

Fig. 7. CMOS Circuit implementation of sensor interface.

In order to measure charge time of capacitors, a comparator has been used to convert charge time to pulse width. If two comparators were used, matching could be a problem. In order to avoid mismatch one comparator is used for converting charge time to pulse width. The output of the comparator is a variable pulse width that its width is proportional to sensor capacitance. Since, the output pulse width is alternatively proportional to sensor and dummy capacitance, the main clock *clk* has been used to separate pulses. The high level of the clock signal *clk* indicates the pulse width for sensor capacitance and low state of the clock signal shows the pulse width for dummy sensor. Therefore, combination of these two signals has been used to measure sensor capacitance change. In order to convert pulse width to digital counts, an up-down counter has been used. The clock *clk* signal is connected to *Up/Dn* control pin of the counter and the sensor output pulse width is connected to the counter enable input *En*. Therefore, when *clk* signal is high the counter will count up the width of sensor pulse and when *clk* is low the sensor will count down for the duration of dummy sensor capacitance pulse width. The resolution of the counter and number of bits used can be adjusted for the required application. If the system is used for detection only, the resolution of the counter can be minimized; therefore, the number of flip-flops used is at minimum for the counter.

4. Simulations and Discussions

Fig. 8 shows simulation waveforms of the voltages across active and dummy sensors. When one sensor is charging the other is at zero voltage and discharged by an NMOS switch. When the charging sensor voltage reaches reference voltage the output of the comparator changes its state. The charging time depends on the current source value and the sensor capacitance.

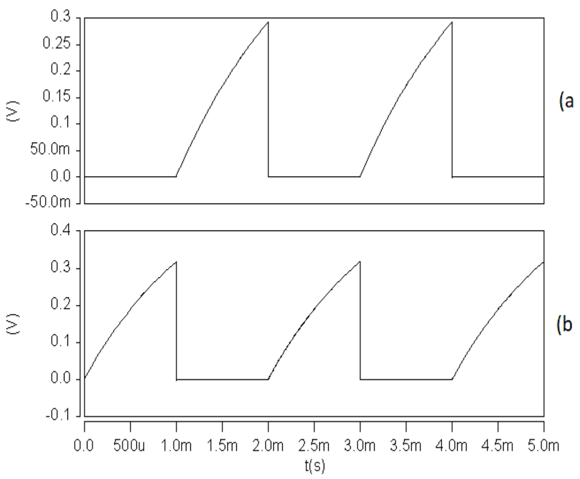

Fig. 8. Simulation waveforms of the sensor: a) Active sensor; b) Dummy sensor.

Fig. 9 shows comparator input and output waveforms. Combination of active and dummy sensor voltages is applied to one input of the comparator (each sensor in T/2 of the clock cycle). The output pulse duration of the comparator is proportional to charging time of each sensor capacitance. A plot of pulse width change versus difference of sensor and dummy capacitances have been shown in Fig. 10. The plot shows good linearity of 0.9 % on average in the capacitance to time conversion in the circuit for 10 pF change in capacitance value.

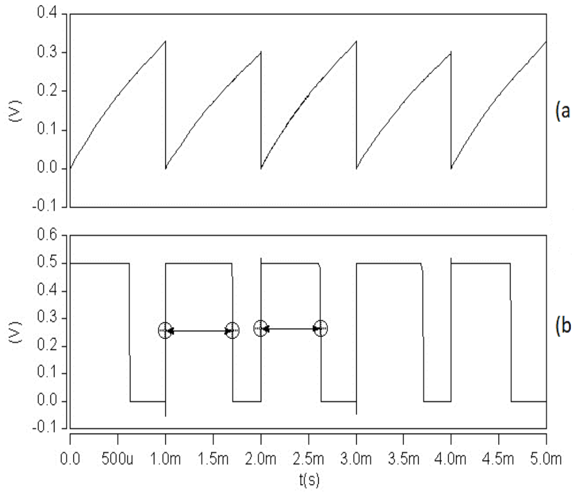

Fig. 9. Comparator pulse width versus capacitance difference.

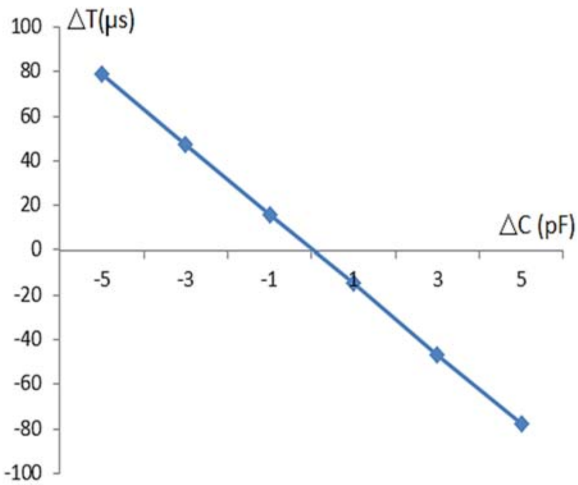

Fig. 10. Pulse duration versus sensor capacitance change.

Table 1 compares the proposed interface circuit with previous reports for capacitance measurement of LC sensor. The proposed circuit offers smaller chip area with very low power consumption and acceptable resolution. When array sensor implementation is desired, interface circuit area and power consumption are of great importance that are well met in the new proposed design. The interface circuit with very small chip area can be repeated hundred times for hundred identical sensor pairs.

Table 1. Comparison of the reported circuits for LC interface.

Ref. #	Technology	Resolution	Power Diss.	Area
[5]	CMOS/0.5 µm	15 aF	1 mW	0.4 mm^2
[6]	a-Si:H/8 µm	-	35 µW	0.02 mm^2
This work	CMOS/90 nm	40 fF	0.2 µW	5.5 μm^2

5. Conclusions

A low power, low voltage sensor interface circuit for LC chemical and biological sensors has been presented. The new array design uses smaller chip area and has lower power consumption, while operating from a single 0.5 V supply voltage. Differential structure removes any unwanted parasitic environmental effects such as temperature change on sensor operation. Direct capacitance to time duration and then to digital conversion is performed that can be repeated for array of sensors operation. Threshold of contamination detection can be easily implemented in the counter section of the circuit by using a preset value for the counter. Auto zero and offset cancellations have been performed using incremental value for the counter. The previous counter value can be preloaded to the counter so the measurement will be subtracted from the next phase value. Low power consumption and array operation are vital for the new generation of chemical and biological sensors, where false detections are minimized. A minimum set of sensors in array should confirm agent detection, before the decision is made for agent presence. The proposed circuit meets low power and small chip area per channel of 5.5 μm^2 for array sensor interface. Simulations have been performed using HSPICE simulation software and TSMC 90 nm technology parameters.

References

[1]. V. K. Gupta, T. B. Dubrovsky, N. L. Abbott, Optical amplification of ligand-receptor binding using liquid crystals, *Science*, Vol. 279, Issue 5359, 1998, pp. 2077–2080.

[2]. J. Brake, M. Daschner, N. L. Abbott, Biomolecular interactions at phospholipid decorated surfaces of thermotropic liquid crystals, *Science*, Vol. 302, Issue 5653, 2003, pp. 2094–2097.

[3]. R. G. Lindquist, A. Abu-Abed, C. Woo-Hyuck, Liquid crystal sensors with capacitive transduction, in *Proceedings of the IEEE 5th Conf. Sensors*, Daegu, Korea, 2006, pp. 1341–1344.

[4]. A. Abu-Abed, R. G. Lindquist, W.-H. Choi, Capacitive transduction for liquid crystal based sensors part1: Orderedsystem, *IEEE Sensors Journal*, Vol. 7, Issue 12, Dec. 2007, pp. 1617–1624.

[5]. A. Hassanzadeh, R. G. Lindquist, Liquid crystal sensor microchip, *IEEE Sensors J.*, Vol. 12, Issue 5, 2012, pp. 1536-1544.

[6]. A. Hassanzadeh, R. G. Lindquist, D. Shen, Design of an a-Si:H interface circuit for liquid crystal chemical and biological sensor array, *IEEE Sensors Journal*, Vol. 12, Issue 5, 2012, pp. 1284-1288.

[7]. S.-T. Wu, D.-K. Yang, Fundamentals of Liquid Crystal Devices, *John Wiley & Sons*, New York, 2006.

[8]. A. Hassanzadeh, Y. Zou, R. G. Lindquist, The effects of excitation signal on the resolution of the liquid crystal capacitive chemical and biological sensors, *IJE Trans. B: Applications*, Vol. 26, Issue 11, 2013, pp. 1275-1280.

[9]. D.-S. Lee, H. Tiwari, S.-Y. Kim, J. Lee, H.-G. Park, Y. Pu, M. Seo, K.-Y. Lee, A Highly Linear, Small-Area Analog Front End With Gain and Offset Compensation for Automotive Capacitive Pressure Sensors in 0.35 µm CMOS, *IEEE Sensors Journal*, Vol. 15, Issue 3, March 2015, pp. 1967-1976.

[10]. K.-T. Lai, Y.-T. Yang, B.-J. Chen, C.-J. Shen, M.-F. Shiu, Z.-C. He, H. C. Chang, C.-Y. Lee, A 3.3V 15.6b 6.1pJ/0.02 Response Humidity Sensor for Respiratory Monitoring, in *Proceedings of the IEEE Asian Solid-State Circuits Conference (A-SSCC)*, November 2014, pp. 293–296.

[11]. A. K. George, J. Lee, Z. H. Kong, M. Je, A 0.8V supply and temperature insensitive capacitance to digital converter in 0.18 µm CMOS, *IEEE Sensors Journal*, Vol. 16, Issue 13, 2016, pp. 5354-5364.